

# MULTISENSOR ANALYSIS OF DISCREPANCIES BETWEEN VEGETATIVE VIGOR AND GRAIN YIELD IN PRECISION MAIZE CROP MANAGEMENT

**Flávio Vanoni de Carvalho Júnior**

Federal University of Lavras, Agricultural Engineering Department, Campus, ZIP Code 37.200-900, Lavras, MG, Brazil

**Marcelo de Carvalho Alves**

Federal University of Lavras, Agricultural Engineering Department, Campus, ZIP Code 37.200-900, Lavras, MG, Brazil

**Gabrielly Carvalho de Souza**

Federal University of Lavras, Agricultural Engineering Department, Campus, ZIP Code 37.200-900, Lavras, MG, Brazil

Corresponding author: gcsouza003@gmail.com

**Fortunato Silva de Menezes**

Federal University of Lavras, Physics Department, Campus, ZIP Code 37.200-900, Lavras, MG, Brazil

**Abstract:** Imagery from sensors embedded in satellites enables low-cost crop analysis and has been the subject of correlation studies between vegetation indices and productivity. Vegetation indices obtained from orbital platforms and crop maps have been important tools in the context of popularizing precision agriculture. However, there are many factors that affect maize yields and the resulting harvest maps. As a result, correlations between vegetation indices and yields are not always obtained. This leaves a gap for methodologies to identify areas of non-correlation and investigate the possible causes in a targeted manner. The aim of this study was to use freely available satellite images, together with yield data from a maize harvester, to identify regions with and without a correlation between yields and vegetation indices. In areas with correlation, a linear model of yield as a function of NDVI was obtained. A map of discrepancies was calculated, in which most of the crop was correlated, with yields varying by around  $2 \text{ Mg ha}^{-1}$  in relation to the model. Areas with discrepant yields were identified, both negatively and positively in relation to the model, enabling a localized investigation into the possible causes of the phenomenon and crop management.

**Keywords:** Remote sensing, Precision agriculture, Sentinel-2, Landsat-8, Vegetation index.

Received: January 10, 2024 - Accepted: February 17, 2024

---

## INTRODUCTION

Sustainable production is one of the biggest challenges in agriculture, whether in environmental, social or economic terms (BASSO; ANTLE, 2020; NEVES; IMPERADOR, 2022). With the growing demand for food, it is understood that technological advances in production areas increase productivity gains, reducing the environmental impacts of agricultural expansion (PATRÍCIO; RIEDER, 2018; TILMAN et al., 2011). This requires the development of technologies that help make decisions in a precise and agile manner, demanding a clear set of information that

portrays the reality of the agricultural environment, from sowing to harvesting. In this context, Precision Agriculture (PA) is a set of technologies that allow crop management at strategic points, since productivity can vary spatially and temporally, reducing input costs and increasing sustainability (GEBBERS; ADAMCHUK, 2010; KENDALL et al., 2022; WHELAN; MCBRATNEY, 2000).

Maize (*Zea Mays* L.) is an important crop distributed in several countries around the world and is used both as a source of food and as a raw material for industry, such as in the production of corn ethanol, which has been growing in Brazil (YANG et al., 2021; COLUSSI et al., 2023).

The country is currently the world's third largest producer and the current scenario is optimistic for producers (COELHO, 2023; HUANG, 2021). Maize yield is influenced by several factors, such as climatic conditions, biological conditions and soil fertility, as well as the quality and genetic adaptability of the plants (ARAÚJO et al., 2016; SHARMA et al., 2022; WADE et al., 2020). In addition, pest attacks can lead to a total loss of production (TIMBÓ; MENEZES; LIMA, 2023). Vegetative vigor, i.e. the ability of plants to grow and develop, is also an important indicator of productivity. Assessing vegetative vigor is a challenge, as plants may only show visible differences at advanced stages of development. Traditional assessment techniques, such as counting leaves or measuring plant height, require field research and are laborious as well as subjective (BERTOLIN et al., 2017). The multisensor approach on an orbital platform has been widely used in studies aimed at quantifying biophysical indices and monitoring vegetation (SANTOS et al., 2020), enabling the study of the correlation between these indices and grain yield (HENRIQUES et al., 2021).

In view of the countless advantages offered by advances in Precision Agriculture in grain harvesting operations, many producers have opted to purchase machines that already come with a complete package of computerized resources to monitor the mechanisms that integrate the machine. In grain harvesters, flow sensors or load cells measure the mass of grain that passes through the grain elevator, which takes it from the tracks to the bulk tank (ALBARENQUE; VÉLEZ, 2011). This equipment, coupled with positioning systems, generates the yield map. This mapping is one of the main sources of information for precision agriculture (MICHELAN; SOUZA; URIBE-OPAZO, 2007). In terms of production factors, it is the most complete information for visualizing the spatial variability of crops (MOLIN, 2002).

In many cases, the relationship between vegetation indices and productivity shows a low correlation due to factors that go beyond the spectral response captured by remote sensing indices. In addition, yield data from harvesters is subject to errors caused by the machine's

own automated yield measurement system (MENEGATTI; MOLIN, 2004; MICHELAN; SOUZA; URIBE-OPAZO, 2007). Therefore, determining zones where vegetation indices and yields are discrepant allows for a localized investigation of variability and the occurrence of phenomena in the area or on the equipment that affect production.

The aim of this study is to evaluate the correlation between vegetation indices calculated from satellite images and the spatial distribution of maize yield, defining areas with or without correlation and thus producing a map of discrepancies in order to identify areas of the crop with yields that differ from what was expected for its vegetative vigor. The objective of this study is to propose and evaluate a methodology for determining the map of discrepancies, providing support for investigations into the causes of lower or higher than expected yields in maize crop.

## MATERIAL AND METHODS

### Study area characterization

This study was performed in the municipality of Cruzília, in the southern region of the state of Minas Gerais, in a field located at 21°40'30" south latitude and 44°45'54" west longitude. Figure 1 shows the location of the perimeter studied in Cruzília, Minas Gerais, in natural RGB composition from the Sentinel-2 satellite imagery. The area under study, known as the *Mata da Fazenda Cachoeira* field, is approximately 52.2 ha in size and the maize variety used was Pioneer's 30F53 VYHR. Elevation in the area varied approximately between 1012 m and 1097 m. In a study carried out by Sá Júnior et al. (2012), the climate class is Cwb (humid temperate climate with dry winter and moderately hot summer) according to the Köppen climate classification. There is minimal climate data available in the neighborhood. According to information obtained from the HIDROWEB (ANA, 2023) rain gauge station of the Instituto Mineiro de Gestão das Águas (IGAM-MG), located 37 km away in the municipality of Aiuruoca, the average annual rainfall was 1425 mm in the period 1990-2020.

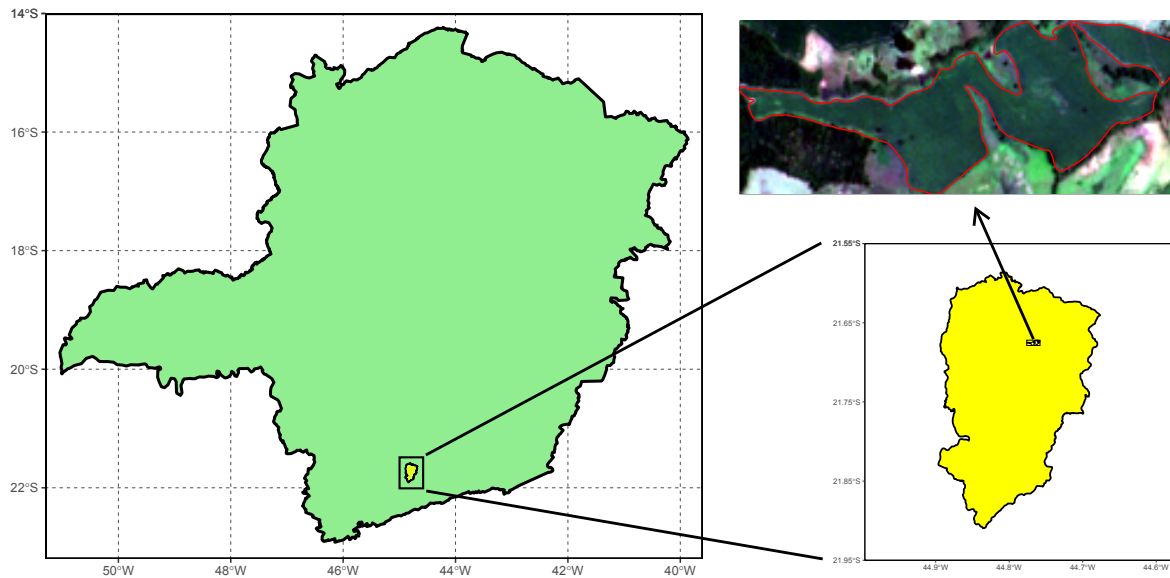


**Figure 1:** Study area location using natural composition RGB 10 m imagery from the Sentinel-2 satellite.

Harvesting in the area began on April 5, 2021 and ended on April 29, 2021. Productivity data was recorded by the John Deere model S760 grain harvester, with 325 hp of nominal power and 10600 L of bulk capacity. Work and performance information is shown in Table 1.

**Table 1:** Operational variables of the John Deere S760 harvester (1 Mg = 1000 kg).

Variable	Values
Area Harvested	52.2 ha
Net Yield	11.3 Mg ha <sup>-1</sup>
Net weight	590 Mg
Moisture	19%
Gross Yield	11.9 Mg ha <sup>-1</sup>
Gross Weight	619 Mg
Speed	3.3 km h <sup>-1</sup>
Productivity	1.7 ha h <sup>-1</sup>
Working Time	30 h 36 min
Total Fuel	1289 L
Yield (Dry)	19.3 Mg h <sup>-1</sup>
Yield (Wet)	20237.2 kg h <sup>-1</sup>
Fuel Efficiency	0.5 Mg L <sup>-1</sup>
Fuel	24.6 L ha <sup>-1</sup>
Fuel	42 L h <sup>-1</sup>

## Harvest data and yield map

The harvester machine John Deere had to be coupled with the precision agriculture technology package and, when harvesting began, the operator had to fill in the data for

the operation, i.e. crop, seed variety, name of the owner, farm and plot. The harvester has several sensors that need to be calibrated. The scale sensor which registers the mass of grain entering the machine is very sensitive, and some factors can alter the result generated in the yield maps, such as the shaking of the ground, the vibration generated by the sieves, among others. Calibrating the harvester's scales is a difficult and time-consuming job, so John Deere software provides calibration after harvest. Post-calibration can be carried out using the productivity obtained from a field that actually arrived at the storage unit. After harvesting, the information was collected using a USB pendrive and inserted into the software for calibration and export the geographic database in shapefile format.

The point vector data obtained by the precision agriculture system includes a geodesic coordinate system, geometry and attributes. The attributes used were productivity in Mg ha<sup>-1</sup> and moisture on a wet basis given as a percentage. The productivity (P) of each point was corrected to 13% wet basis moisture according to Equation 1. The correction is necessary because the grain moisture in the field is variable. The value of 13% is adopted because this is a desirable humidity for safe storage. Grains with high humidity lose mass during drying, therefore Equation 1 allows determining

the productivity value when the grains reach 13% humidity on a wet basis.

$$P(13\%) = P \frac{100 - \text{Moisture} (\%)}{100 - 13} \quad (1)$$

The yield points are recorded every approximately 1 m as the harvester moves forward and represent what has been harvested in an area the width of the harvesting platform by the distance traveled. For the analysis, this spatial points needs to be transformed into raster data using an appropriate process. The points were transformed into pixels using the rasterize function in the terra package (HIJMANS et al., 2023). Applying this function requires the creation of a base raster with the desired size and resolution. A base raster (without values) was created for the extent of the crop, with  $\frac{10}{32}$  m resolution and the rasterize function was applied to the spatial points, informing the attribute (YIELD) to be rasterized, as shown in Figure 2. This resolution was adopted in order to promote good precision in the positioning of pixels in relation to their original points. Furthermore, as the raster must have the same extension and resolution as the NDVI for the regression to be possible, the base raster was created by dividing the 10 m resolution by a fixed factor, in this case 32. This makes it possible to aggregate the raster with factor = 32 to result in 10 m resolution. In the same way, when aggregating with a factor of 96, a resolution of 30 m is obtained to be used with the Landsat-8 data. The mean function is applied so that if there are two or more yield points within a pixel, the pixel is composed of the average of these points. The raster obtained was then used to apply the focal function of the terra 1.7.29 package (HIJMANS et al., 2023). This function calculates values for each cell using a statistic of the neighborhood contained in a weight matrix, called moving window. A 3x3 cross-shaped matrix with weight 1 (see Figure 2) was used to compute the neighborhood values of the yield pixels. The cross format of the matrix was adopted so that during the passage of the "moving window", pixels in the diagonal directions of the cell's neighborhood would not be used. Therefore, only perpendicular pixels are used in the focal computation because they

are the closest neighbors. When more than one value is obtained within the moving window, the fun=mean argument allows these values to be averaged to compute the cell value. By applying the focal function multiple times, the space between the yield pixels is filled by the nearest neighbor or the average of the nearest neighbors. As shown in Figure 2, the focal function was applied using the arguments na.rm=TRUE to remove NA values from the focal computation and na.policy='only' to insert values only in NA cells. We adopted 25 repetitions in the iteration structure, but the minimum value required may vary depending on the maximum distance between the points. The raster was aggregated with the aggregate function from the terra package for 10 m and 30 m by average. Figure 3 illustrates in a simplified way the process of preparing the harvest map, starting with the vector data (points) (Figure 3a) followed by its rasterization into a base raster (Figure 3b). The focal function applied several times fills the empty spaces by averaging the values of the cross-shaped moving window (Figure 3c). After applying the aggregate function, the pixels are aggregated to 10 m spatial resolution by averaging their values (Figure 3d).

```
Rast <- rasterize(Prod, raster_base,
                  "YIELD", fun=mean)

w <- matrix(
  data=c(NA, 1, NA,
         1, 1, 1,
         NA, 1, NA),
  nrow=3, ncol=3) #Moving window

for(i in 1:25) {
  Rast <- focal(Rast, w,
               fun=mean, na.rm=TRUE,
               pad=TRUE,
               na.policy='only')
}

Rast10m <- aggregate(
  Rast, fun="mean", fact = 32) #To 10 m
Rast30m <- aggregate(
  Rast, fun="mean", fact = 96) #To 30 m
```

Figure 2: Example of code chunk with functions used in the R console to create thematic yield map.

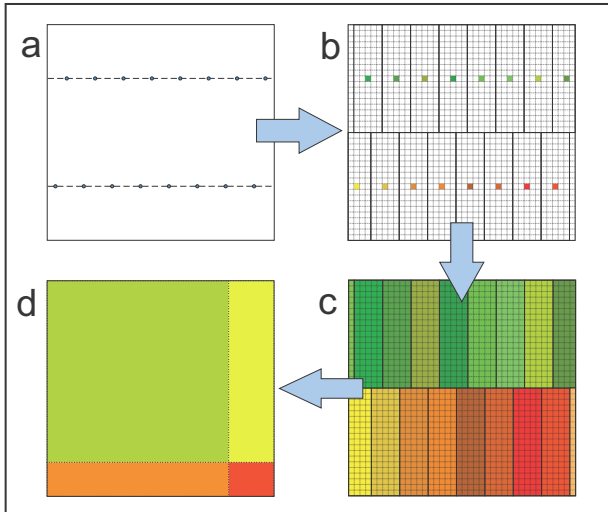


**Figure 3:** Harvest map preparation process. Pixel colors refer to attribute values of maize yield in the field.

## Vegetation indices

Surface reflectance images of the study area were obtained on January 31, 2021 from the Sentinel-2 (ESA, 2023) satellite and February 4, 2021 from the Landsat-8 (USGS, 2023) satellite acquired from the Copernicus Open Access Hub and Earth Explorer portal, respectively. The images were selected with acquisition dates close to and before the harvest, which began on April 5, 2021. The Sentinel-2 satellite images have 10 m spatial resolution for the Red and NIR bands and 20 m for the Red Edge 2 band, while the Landsat-8 satellite images have 30 m spatial resolution. All image processing was performed in the R environment.

The NDVI vegetation index (Normalized Difference Vegetation Index) (Equation 2) (ROUSE et al., 1973) and the NDRE index (Normalized Difference Red Edge Vegetation Index) (GITELSON; MERZLYAK, 1994) were used. Both indices were calculated for Sentinel-2 satellite data and only NDVI for Landsat satellite data. The Sentinel-2 satellite provides four red edge bands at different wavelengths. The NDRE was obtained using the same equation as the NDVI, replacing the Red band (B04 - 665 nm) with Red Edge 2 (B06 - 740 nm), resampled to 10 m resolution by bilinear interpolation for the calculation (Equation 3).

$$\text{NDVI} = \frac{\rho_{\text{nir}} - \rho_{\text{red}}}{\rho_{\text{nir}} + \rho_{\text{red}}} \quad (2)$$

$$\text{NDRE} = \frac{\rho_{\text{nir}} - \rho_{\text{red edge}}}{\rho_{\text{nir}} + \rho_{\text{red edge}}} \quad (3)$$

## Correlation and discrepancy analyses

A visual representation of the vegetation indices and the harvest raster was obtained for the visual correlation analysis using the stars package (PEBESMA, 2022) in R. The same color palette and scientific geovisualization techniques were used to visually identify areas with a correlation between the vegetation indices and yield.

Five polygons were delimited in areas that showed the greatest visual correlation between NDVI and yield. The maize grain yield raster and the NDVI raster were masked by the five polygons. This resulted in a linear regression of productivity as a function of NDVI in the areas delimited by the five polygons.

The equation obtained from the linear model was used to generate a map estimating yield as a function of NDVI. Using map algebra, the difference between productivity and the estimate map was calculated. The resulting raster was represented so that the areas with positive and negative yield discrepancies could be seen.

## RESULTS AND DISCUSSION

### Vegetation indices and harvest map

The NDVI indices from the Sentinel-2 and Landsat-8 satellites are shown in Figure 4. Both indices showed a very similar spatial distribution in the area, except for the greater detail provided by the 10-meter spatial resolution of Sentinel-2. In the case of the NDRE (Figure 4), despite being represented with 10 meters of spatial resolution, the result is derived from a band with 20 meters of resolution. Because the Sentinel-2 RedEdge band has 20 meters of resolution, it had to be resampled to 10 meters. This resulted in a loss of detail in relation to the NDVI calculated with the native 10 m bands. As for the NDVI from Landsat-8, we observed variability in the area, but with a certain limitation imposed by the spatial resolution.

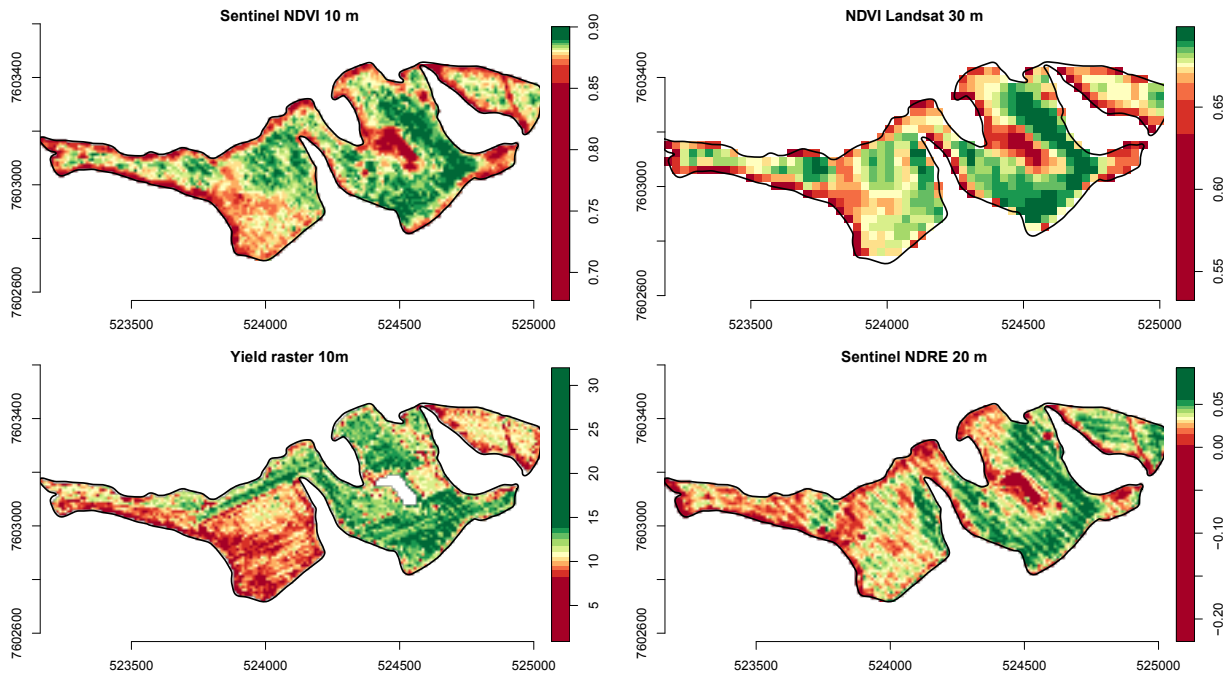


**Figure 4:** Vegetation indices and yield maps of mechanical maize harvesting using precision agriculture techniques ( $Mg\ ha^{-1}$ ).

### Delineating correlation polygons

Figure 5 shows the polygons delimited on the harvest map, in areas where we observed a visual correlation between productivity and vegetation indices. Each polygon is approximately half a hectare in size and has been arranged to cover all the maize fields. The linear

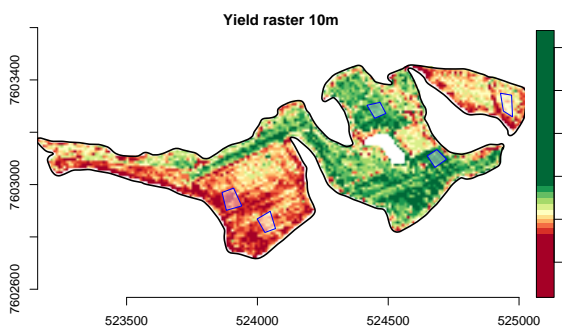


**Figure 5:** Spatial polygons defined on the yield map for statistical modeling.

regression fits of yield as a function of NDVI for data from two satellites are shown in Figure 6. The correlation was strong for Sentinel-2 and moderate for Landsat-8, with determination coefficients ( $R^2$ ) of 0.708 and 0.590, respectively. Some areas showed a clear relationship between increases and decreases in yield as a function of

NDVI, while in others there was no relationship at all. Studies involving the correlation between vegetation indices and maize yield show quite varied results. This is due to the fact that many factors can interfere yield in addition to green biomass, such as plant nutrition conditions, pest attacks and the consumption of produce by local fauna. In the case of maize safrinha (off-season), there is greater susceptibility to attack by pests compared to the first crop (safra), mainly due to climatic conditions. It should be noted that maize is attacked by pests and diseases throughout the entire development period, from sowing to harvest (WORDELL FILHO et al., 2016). Attack on grains is a major cause of production losses (PICANÇO et al., 2003). Therefore, the possibility of losses due to pest attacks in the reproductive phase of the crop should be considered, at times after the images have been acquired. Another source of discrepancies is the errors inherent in the data collected by the harvesters' automated systems (MENEGATTI; MOLIN, 2004).

The strong correlation obtained within the delimited polygons shows that vegetation indices do indeed influence yields. The best results for the data from the Sentinel-2 satellite are largely due to the 10-meter spatial resolution,

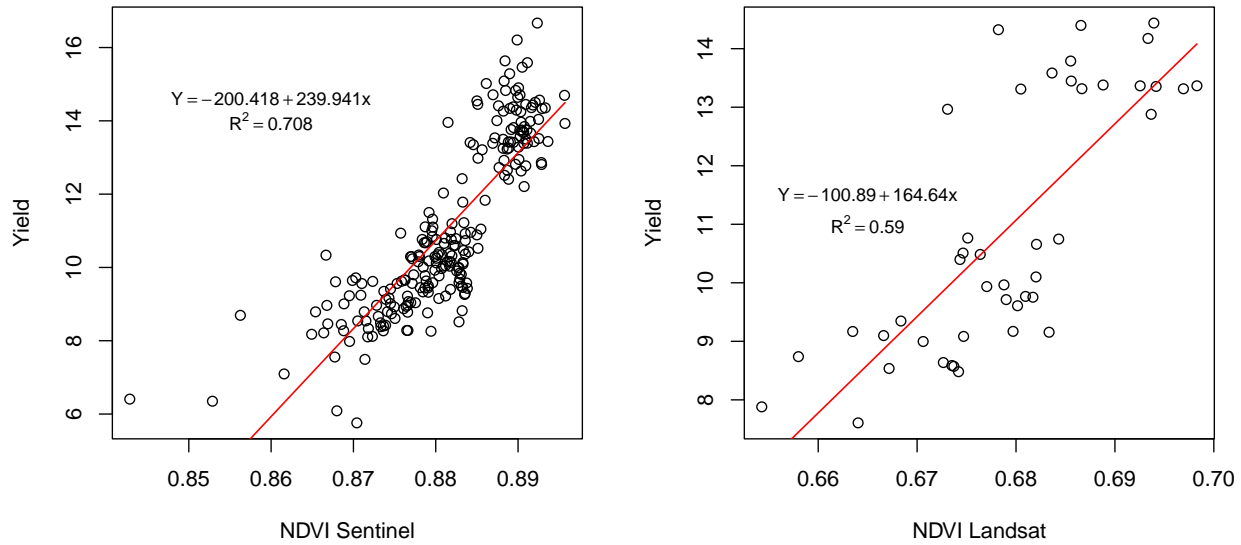


**Figure 6:** Linear regression of NDVI as a function of yield ( $Mg\ ha^{-1}$ ) in the spatial polygons used in the modeling (showed on Figure 5).

providing greater detail of the area compared to Landsat-8. Especially when you consider the fact that the area is relatively small and located in a region with more rugged terrain, where spatial variations in climatic and soil attributes tend to be greater. It is known that in general the temperature varies linearly by  $-0.6^{\circ}C$  with an increase of 100 meters in altitude (HIRASUGA; LEUNG, 2019) and that soil attributes vary both horizontally and vertically (RICHTER et al., 2011).

**Table 2:** Summary statistics for variations between yield measured in the field and determined by modeling.

Summary statistics	values ( $Mg\ ha^{-1}$ )
Min.	-9.414
1st Qu.	-1.154
Median	0.370
Mean	0.796
3rd Qu.	1.973
Max.	30.242
SD	3.102
NA's	8600

## Implementing the model and discrepancy map

The green areas in Figure 7 represent those where the difference between the yield and the NDVI-based model was between  $-2$  and  $2\ Mg\ ha^{-1}$ . In light blue to purple are the areas where the yield was considerably higher than the model. Yellow to red are the areas where the yield recorded was considerably lower than the model. Some areas showed visible discrepancies, while most of the area followed the model. The mean discrepancy in the area was  $0.80\ Mg\ ha^{-1}$  positive, while 75% of the values were between  $-1.15$  and  $1.97\ Mg\ ha^{-1}$  (Table 2). The standard deviation was  $3.10\ Mg\ ha^{-1}$ . In the discrepancy map (Figure 7), most of the area followed the model, but

certain discrepant zones and points scattered throughout the crop meant that the level of correlation was greatly reduced. Analysis of the map obtained allows us to investigate areas of positive and negative divergence, providing information to determine possible causes of variability and possible corrective actions.

Yields above the model were found at the edges along much of the area's perimeter. One of the possible causes of the edge effect may be related to the spatial resolution of the satellite images which, because they cover a larger area, end up capturing effects from zones outside the area actually cultivated. The presence of tracks in the middle of the field can cause the same effect. Regions with yields lower than the model should be investigated by the producer to determine the causes of the low yields, which are not always

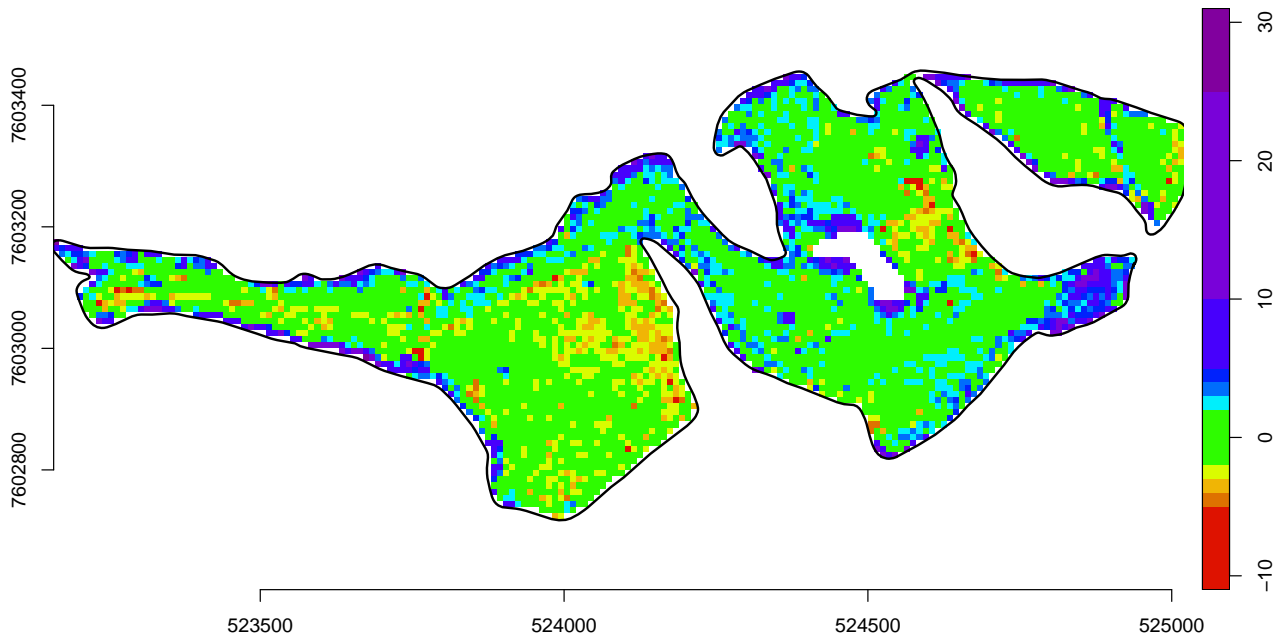


**Figure 7:** Variation between yield measured and determined by modeling ( $Mg\ ha^{-1}$ ).

related to the vegetative vigor reported by the vegetation indices. As an example, planting failures and plant mortality can be hidden after plant growth by the NDVI index.

## CONCLUSIONS

A methodology was developed to analyze yield maps determined *in situ* and assess their accuracy according to satellite crop monitoring data from a crop management perspective.

The spatial variability of NDVI and yield was visualized with the data collected in the maize field. We identified areas in the field with a strong correlation between maize yield and NDVI and specific locations where there was no correlation.

The NDVI index from Sentinel-2, with 10 meters of spatial resolution, performed better at capturing variability than the 30-meter NDVI from Sentinel-2 and the NDRE calculated from 20-meter spatial resolution data from Sentinel-2.

Using the model applied to produce the discrepancy map enabled to identify areas with divergent values in which factors other than vegetative vigor captured by NDVI affected the area, as well as the incidence of errors in the harvest data, providing information for the producer to act in a localized manner.

Further studies are needed to apply the method to different production areas and crop phenological stages, combined with field research and climate data in order to identify causes of discrepancies.

## REFERENCES

- ALBARENQUE, S. M.; VÉLEZ, J. P. **Técnicas para el procesamiento de mapas de rendimiento**. 1. ed. Yuto: Ediciones INTA, 2011.
- ANA, Agência Nacional de Águas e Saneamento Básico. **HIDROWEB v3.2.7**. 2023. Available from: <<https://www.snirh.gov.br/hidroweb/serieshistoricas>>. Visited on: 1 Jan. 2024.
- ARAÚJO, L. S. et al. Desempenho agrônomo de híbridos de milho na região sudeste de Goiás. **Agro@ambiente On-line**, v. 10, n. 4, p. 334–341, 2016. DOI: 10.18227/1982-8470ragro.v10i4.3334.
- BASSO, B.; ANTLE, J. Digital agriculture to design sustainable agricultural systems. **Nature Sustainability**, v. 3, n. 4, p. 254–256, 2020. DOI: 10.1038/s41893-020-0510-0.
- BERTOLIN, N. et al. Predição da produtividade de milho irrigado com auxílio de imagens de satélite. **Revista Brasileira de Agricultura Irrigada**, v. 11, n. 4, p. 1627–1638, 2017. DOI: 10.7127/rbai.v11n400567.

- COÊLHO, J. D. Agricultura: Milho. **Caderno Setorial**, v. 8, n. 283, p. 1–9, 2023. p. 319–351, 2022. DOI: 10.1007/s11119-021-09839-2.
- COLUSSI, J. et al. Brazil Emerges as Corn-Ethanol Producer with Expansion of Second Crop Corn. **farmdoc daily**, v. 13, n. 120, p. 1–5, 2023. Available from: <<https://farmdocdaily.illinois.edu/2023/06/brazil-emerges-as-corn-ethanol-producer-with-expansion-of-second-crop-corn.html>>.
- ESA, European Space Agency -. **Sentinel-2 Level-2**. 2023. Available from: <<https://sentinels.copernicus.eu/web/sentinel/user-guides/sentinel-2-msi/processing-levels/level-2>>. Visited on: 17 Nov. 2023.
- GEBBERS, R.; ADAMCHUK, V. I. Precision Agriculture and Food Security. **Science**, v. 327, n. 5967, p. 828–831, 2010. DOI: 10.1126/science.1183899.
- GITELSON, A. A.; MERZLYAK, M. N. Quantitative estimation of chlorophyll-a using reflectance spectra: experiments with autumn chestnut and maple leaves. **Journal of Photochemistry and Photobiology B: Biology**, v. 22, n. 3, p. 247–252, 1994. DOI: 10.1016/1011-1344(93)06963-4.
- HENRIQUES, H. J. R. et al. Vegetation indices and their correlation with second-crop corn grain yield in Mato Grosso do Sul, Brazil. **Brazilian Journal of Maize and Sorghum**, v. 20, e1195, p. 1–13, 2021. DOI: 10.18512/rbms2021v20e1195.
- HIJMANS, R. J. et al. **Package ‘terra’**. 2023. Available from: <<https://cran.r-project.org/web/packages/terra/terra.pdf>>.
- HIRASUGA, N.; LEUNG, L. Using computer climate generator versus conventional lapse rate to model skyscrapers. **Earth and Environmental Science**, v. 294, n. 012038, p. 1–10, 2019. DOI: 10.1088/1755-1315/294/1/012038.
- HUANG, F. Resistance of the fall armyworm, *Spodoptera frugiperda*, to transgenic *Bacillus thuringiensis* Cry1F corn in the Americas: lessons and implications for Bt corn IRM in China. **Insect Science**, v. 28, p. 574–589, 2021. DOI: 10.1111/1744-7917.12826.
- KENDALL, H. et al. Precision agriculture technology adoption: a qualitative study of small-scale commercial “family farms” located in the North China Plain. **Precision Agriculture**, v. 23, n. 1, p. 319–351, 2022. DOI: 10.1007/s11119-021-09839-2.
- MENEGATTI, L. A. A.; MOLIN, J. P. Remoção de erros em mapas de produtividade via filtragem de dados brutos. **Revista Brasileira de Engenharia Agrícola e Ambiental**, v. 8, n. 1, p. 126–134, 2004. DOI: 10.1590/S1415-43662004000100019.
- MICHELAN, R.; SOUZA, E. G.; URIBE-OPAZO, M. A. Determinação e remoção do tempo de atraso em mapas de colheita de milho. **Acta Scientiarum. Agronomy**, v. 29, n. 2, p. 147–155, 2007. DOI: 10.4025/actasciagron.v29i2.337.
- MOLIN, J. P. Definição de unidades de manejo a partir de mapas de produtividade. **Engenharia Agrícola**, v. 22, n. 1, p. 83–92, 2002.
- NEVES, J. A.; IMPERADOR, A. M. The agroecological transition: challenges for sustainable agriculture. **Revista GEAMA, Scientific Journal of Environmental Sciences and Biotechnology**, v. 8, n. 3, p. 5–14, 2022.
- PATRÍCIO, D. I.; RIEDER, R. Computer vision and artificial intelligence in precision agriculture for grain crops: A systematic review. **Computers and Electronics in Agriculture**, v. 153, p. 69–81, 2018. ISSN 0168-1699. DOI: 10.1016/j.compag.2018.08.001. Available from: <<https://www.sciencedirect.com/science/article/pii/S0168169918305829>>.
- PEBESMA, Edzer. **stars: Spatiotemporal Arrays, Raster and Vector Data Cubes**. 2022. Available from: <<https://r-spatial.github.io/stars/>>.
- PICANÇO, M. C. et al. Intensities of losses and of insect pests attack to cultivars on the late maize cultivation. **Ciênc. agrotec.**, v. 27, n. 2, p. 339–347, 2003. DOI: 10.1590/S1413-70542003000200013.
- RICHTER, R. L. et al. Variabilidade espacial de atributos da fertilidade de um latossolo sob plantio direto influenciados pelo relevo e profundidade de amostragem. **Enciclopédia Biosfera**, v. 7, n. 13, p. 1043–1059, 2011.
- ROUSE, J. W. et al. Monitoring vegetation systems in the Great Plains with ERTS. In: **PROCEEDINGS OF THE 3RD. ERTS-1 SYMPOSIUM**, p. 309–316.
- SÁ JÚNIOR, A. et al. Application of the Köppen classification for climatic zoning in the state of Minas Gerais, Brazil. **Theoretical and Applied Climatology**, v. 108, p. 1–7, Apr. 2012. DOI: 10.1007/s00704-011-0507-8.

SANTOS, R. Argolo dos et al. Remote sensing as a tool to determine biophysical parameters of irrigated seed corn crop. **Semina: Ciências Agrárias**, v. 41, n. 2, p. 435–446, 2020. DOI: 10.5433/1679-0359.2020v41n2p435.

SHARMA, R. Kumar et al. Impact of recent climate change on corn, rice, and wheat in southeastern USA. **Scientific Reports**, v. 12, n. 16928, p. 1–14, 2022. DOI: 10.1038/s41598-022-21454-3.

TILMAN, D. et al. Global food demand and the sustainable intensification of agriculture. **PNAS**, v. 108, n. 50, p. 20260–20264, 2011. DOI: 10.1073/pnas.1116437108.

TIMBÓ, F. V. A. M.; MENEZES, T. A.; LIMA, R. P. Main pests that affect corn crops. **Revista Foco**, v. 16, n. 10, p. 1–17, 2023. DOI: 10.54751/revistafoco.v16n10-187.

USGS. **Landsat Collection 2 Level-2 Science Products**. 2023. Available from: <<https://www.usgs.gov/landsat-missions/landsat-collection-2-level-2-science-products>>. Visited on: 17 Nov. 2023.

WADE, J. et al. Improved soil biological health increases corn grain yield in N fertilized systems across the Corn Belt. **Scientific Reports**, v. 10, n. 3917, p. 1–9, 2020. DOI: 10.1038/s41598-020-60987-3.

WHELAN, B. M.; MCBRATNEY, A. B. The “null hypothesis” of precision agriculture management. **Precision Agriculture**, v. 2, n. 3, p. 265–279, 2000. DOI: 10.1023/A:1011838806489.

WORDELL FILHO, J. A. et al. **Pragas e doenças do milho: Diagnose, danos e estratégias de manejo. Boletim técnico N° 170**. Florianópolis: Epagri, 2016. P. 88.

YANG, W. et al. Estimation of corn yield based on hyperspectral imagery and convolutional neural network. **Computers and Electronics in Agriculture**, v. 184, n. 106092, p. 1–10, 2021. DOI: 10.1016/j.compag.2021.106092.